

RSC Advances



This is an *Accepted Manuscript*, which has been through the Royal Society of Chemistry peer review process and has been accepted for publication.

Accepted Manuscripts are published online shortly after acceptance, before technical editing, formatting and proof reading. Using this free service, authors can make their results available to the community, in citable form, before we publish the edited article. This *Accepted Manuscript* will be replaced by the edited, formatted and paginated article as soon as this is available.

You can find more information about *Accepted Manuscripts* in the [Information for Authors](#).

Please note that technical editing may introduce minor changes to the text and/or graphics, which may alter content. The journal's standard [Terms & Conditions](#) and the [Ethical guidelines](#) still apply. In no event shall the Royal Society of Chemistry be held responsible for any errors or omissions in this *Accepted Manuscript* or any consequences arising from the use of any information it contains.

Cite this: DOI: 10.1039/c0xx00000x

www.rsc.org/xxxxxx

ARTICLE TYPE

Application of successive self-nucleation and annealing (SSA) to poly(1-butene) prepared by Ziegler-Natta catalysts with different external donorsTao Zheng^a, Qian Zhou^a, Qian Li^b, Huayi Li^{*b}, Liaoyun Zhang^{*a}, Youliang Hu^b

Received (in XXX, XXX) Xth XXXXXXXXX 20XX, Accepted Xth XXXXXXXXX 20XX
DOI: 10.1039/b000000x

Alkoxy silane compounds $R_1R_2Si(OMe)_2$ were used as an external donor for 1-butene polymerization with $MgCl_2$ supported Ziegler-Natta catalysts. The structure of the prepared iPB was characterized by ^{13}C NMR and GPC. The thermal property of poly(1-butene) (iPB) was studied by DSC. The crystallization behavior and the sequence length distribution of poly(1-butene) were investigated through the successive self-nucleation and annealing (SSA) thermal fractionation technology. The SSA results indicated that the steric hindrance of external donor has more influence on the property of iPB, the each peak of the melting point and the enthalpy of fusion of iPB gradually increased with the increase of steric hindrance of external donor. And considering all properties, cyclopentyl isopropyl dimethoxysilane had better advantage relative to other external donors in the polymerization of 1-butene.

Introduction

The isotactic poly(1-butene) (iPB) showed interesting physical and mechanical properties, such as heat-resistant creep degeneration, good environmental stress cracking resistance performance, and good tenacity. Therefore, the iPB could be used as pipe, film and sheet material, and especially as hot water pipe material^{1,2}.

Isotactic poly(1-butene) was first synthesized by Ziegler-Natta catalysts^{3,4}. Although the catalyst used for preparing PE and PP was similar to that of iPB, the technology of 1-butene polymerization was difficult to implement which leads to higher cost and limits its commercial development. External donor (D_e) was one of important parts of catalyst system during 1-butene polymerization¹. External donor was the key point to achieve isotactic polymer with higher degree of isotacticity⁵ and the desired physico-chemical properties of the product. In recent years, researchers had much concern for alkoxy silane as external donor of Ziegler-Natta catalyst. External donor had more influence on the microstructure of polypropylene^{6,7}. Busico et al.⁸ proposed a three-site model to explain the effects of external donor on catalyst efficiency and polypropylene stereoregularity. In this model, successive adsorption of D_e on catalyst changed the stereochemical environment of the active center, which could turn atactic centers into isotactic centers. This model could also apply to other polyolefins.

Successive self-nucleation and annealing (SSA)⁹⁻¹¹ was regarded as an effective technique to characterize the microstructure of polypropylene. Our research group had studied isotactic sequence length and its distribution of PP prepared by Ziegler Natta catalyst using different alkoxy silanes as external donor using

SSA¹², which could be connected with many macro-properties, such as mechanic, thermal and process properties.

Although there were many reports for the influence of external donor on propylene polymerization and polypropylene, the investigation of the effect of external donor on 1-butene polymerization and poly(1-butene) was few. Kudinova et al.¹³ reported the use of polydentate phosphine oxides as electro donor of $TiCl_4$ - $MgCl_2$ catalysts could obtain highly isotactic poly(1-butene) and the isotactic index could reach 92.4% when the external donor was iso-AmP(O)(CH_2OMe)₂. Hegang Ren et al.¹⁴ studied diphenyl dimethoxysilane or cyclohexyl methyl dimethoxysilane as external donor of $TiCl_4$ - $MgCl_2$ catalysts, which external donor could improve the catalytic activity slightly and sharply increased the isotactic index, and cyclohexyl methyl dimethoxysilane has been found to be more effective electron donor than diphenyl dimethoxysilane.

In this paper, poly(1-butene)s were prepared by Ziegler-Natta catalyst with different external donors. The effects of external donor on the molecular weight, the molecular weight distribution and isotactic index of poly(1-butene) were investigated, especially, SSA technique was first used for studying the microstructure and properties of poly(1-butene).

Experimental**Materials**

$MgCl_2$ -supported Ziegler-Natta catalyst (SAL, Ti content of 2.5%), triethyl aluminum (TEA) and 1-butene (polymerization grade) were provided by YanShan Petrochemical Co. Ltd. Cyclohexylmethyl dimethoxysilane (Donor-C), Diisopropyl Dimethoxysilane (Donor-P), Dicyclopentyl Dimethoxysilane (Donor-D), Dicyclohexyl Dimethoxysilane (Donor-H) and

Cyclopentyltrimethoxysilane (CPTMS) were provided by LuJing Chemical. Isobutylmethyl Dimethoxysilane (Donor-MB), Isopropylmethyl Dimethoxysilane (Donor-MP), Cyclopentylmethyl Dimethoxysilane (Donor-MD), Isobutylisopropyl Dimethoxysilane (Donor-PB) and Cyclopentyl isopropyl Dimethoxysilane (Donor-PD) (Figure 1) were synthesized by our group.

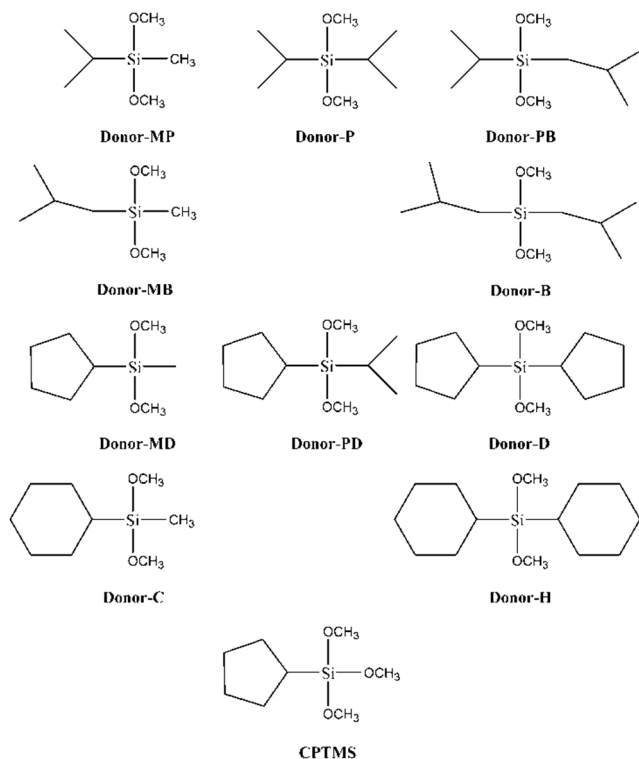


Fig. 1 The structure of external donors with different substituent groups

Polymerization of 1-Butene

In a typical experiment, a 5L of stainless reactor equipped with a mechanical stirrer was degassed at 70°C, and then the Ziegler-Natta catalyst (15mg), TEA (7.92mmol) in n-hexane solution and the alkoxy silane compounds (Si/Ti=20) were added. Then hydrogen (0.04MPa) and 1-butene were charged with the system. The mixture was stirred at a stirring rate of 300 rpm. The autoclave reactor was heated to 40°C and stirred for 60min. Exclude unreacted 1-butene, subsequently, dried under vacuum at 60°C until the weight of the polymer was constant. Catalyst activity was determined in terms of the amount of produced PB (kg) per the amount of catalyst used (g).

Measurement

¹³C NMR spectra of polymers were recorded with a DMX 300M (Bruker). Polymer solution was prepared with 80mg of polymer in 0.5ml deuterated o-dichlorobenzene at 373K.

The molecular weights (M_n and M_w) and the molecular weight distribution (MWD) of samples were determined by a PL-GPC 220 high-temperature gel permeation chromatography at 413K, using 1,2,4-trichlorobenzene as solvent, and the flow rate was 1.0ml min⁻¹. Calibration was made by polystyrene as the standard sample.

Isotacticity of the polymer obtained was determined by extracting

the polymer with boiling ether in a Soxhlet extractor. The boiling ether-insoluble fraction was a crystalline polymer and recognized as iPB. The weight percentage of ether insoluble polymer in a whole sample was reference as isotactic index (I.I.)

Differential scanning calorimetry (DSC) measurements were performed on Q2000 instrument under nitrogen atmosphere. The heating rate was 10°C min⁻¹ range from 40°C to 180°C. The degree of crystallinity was calculated according to the following formula:

$$X_c = \Delta H_m / \Delta H_m^0$$

Where ΔH_m was the fusion heat obtained from DSC curve, ΔH_m^0 (62J/g) was the fusion heat of a perfectly crystalline iPB which crystal was \square^{15} . Then, for the purpose of evaluating the microstructure of the iPB, self-nucleation experiments (SN)^{9, 16, 17} and successive self-nucleation and annealing experiments (SSA)^{17, 18} were employed as follows:

Self-nucleation experiments (SN)

The self-nucleation and annealing experiment using DSC was originally reported by Fillon et al.¹⁹ for isotactic polypropylene (PP).

The successive self-nucleation and annealing (SSA) protocol employed was very similar to that reported previously. The detailed procedure was described as following: (a) Heat the sample to 180°C and maintain such temperature for 5min to erase previous thermal history. (b) Cool the sample to 30°C at 20°C/min to the initial "standard state". (c) Heat at 20°C/min to a selected self-seeding temperature (T_s) located in the final melting temperature range of the sample. (d) The sample was held at this T_s for 5min. This isothermal treatment at T_s results in partial melting and, depending on T_s , in the annealing of unmelted crystals, while some of the melted species may isothermally crystallize (after being self-nucleated by the unmelted crystals). (e) Cool from T_s to 30°C at a rate of 10°C/min; where the effects of SN would be revealed by the crystallization behavior of the sample. (e) Steps "c", "d", and "e" were repeated at progressively lower T_s . The number of repetitions (cycles) can be chosen to cover the entire melting range of the sample with a "standard" thermal history or a shorter range. (f) Finally, heat the sample to 180°C at 10°C/min, where the effect of the entire SN and annealing treatment would also be revealed by the melting behavior of the sample.

Successive self-nucleation/annealing experiments

(a) Heat the sample to 180°C and maintain such temperature for 5min to erase previous thermal history. (b) Cool the sample to 30°C at 20°C/min to the initial "standard state". (c) Heat at 20°C/min to T_s and maintain that temperature for 5min. The first applied T_s temperature was chosen so that the polymer would only self-nucleate (i.e. T_s would be high enough to melt all the crystalline regions except for small crystal fragments that can later self-seed the polymer during cooling). (d) Cool from T_s to 30°C at a rate of 20°C/min. (e) Heat the sample to a new T_s temperature which was 5°C lower than the previous T_s and maintain that temperature for 5min. (f) Repeat steps "d" and "e" until the entire melting range of the original sample was covered. (g) Finally, the sample was heated to 180°C/min at a rate of 10°C/min.

Cite this: DOI: 10.1039/c0xx00000x

www.rsc.org/xxxxxx

ARTICLE TYPE

Table 1 The results of molecular weight and molecular weight distribution of iPB

Samples (or Donor) ^a	Activity (kg·PB·g·cat)	M_n^b (10^4 g/mol)	M_w^b (10^4 g/mol)	M_w/M_n^b	I.I. ^c (%)
Donor-MP	20.4	13.9	46.5	3.36	97.8
Donor-MB	13.3	16.7	48.5	2.90	96.4
Donor-MD	17.7	16.7	53.8	3.22	97.0
Donor-C	9.8	16.1	63.6	3.96	97.0
Donor-P	20.0	32.4	77.2	2.38	97.6
Donor-PB	18.0	25.6	70.2	2.75	98.0
Donor-PD	17.1	27.0	79.1	2.93	98.0
Donor-D	7.3	29.7	92.1	3.09	97.0
Donor-H	3.3	17.0	60.5	3.55	96.2
Donor-B	11.7	25.4	73.5	2.90	97.2
CPTMS	4.5	27.0	81.1	3.01	95.4

^aReaction temperature was 40°C. ^bGel permeation chromatography (GPC) measurements were performed using PL-GPC 220, the solvent was 1,2,4-trichlorobenzene. ^cThe isotactic index.

Results and discussion

5 The external donor showed strong effect on the catalyst activity, isotactic index (I.I.) and molecular weight, as well as molecular weight distribution of iPB. The catalyst activity, molecular weight, the molecular weight distribution and isotactic index (I.I.) of iPB were as shown in Table 1.

10 The catalyst activity was influenced by the structure of external donors. The results could relate with the size and number of alkoxy group, size of hydrocarbon group of alkoxy silane. For the polymerization results, the lowest catalyst activity was obtained by CPTMS and the highest catalyst activity was obtained by Donor-MP and Donor-P. As reported by Seppala et al.^{20, 21}, the most important factor of the catalyst activity and the properties of obtained polymer were the number of alkoxy groups attached to the silicon atom, the more alkoxy groups lead to effectively deactivate the active centers of catalyst. Besides, the size of the hydrocarbon group bonded to the silicon atom was significant factor too. If the hydrocarbon group has the right size, active centers were deactivated selectively, the isotactic index increased. When R₁ was methyl or isopropyl in R₁R₂Si(OMe)₂, with the increase of the R₂ size of external donors, the isotactic degree of iPB showed an increasing trend. A generally accepted mechanism was that alkoxy silane could complex with both the active sites and the cocatalysts (TEA in this work). Bulky substituents on alkoxy silane were required to prevent the external donor from leaving the catalyst surface through complexation with the cocatalyst²², therefore isotactic degree of the obtained iPB was higher. But when the steric hindrance of substituent group of external donors was too big, the complexation became weak, so the isotactic degree of iPB decreased.

The weight-average molecular weight (M_w) was influenced by the structure of external donor. From Table 1, the M_w increased with increasing the size of hydrocarbon groups in external donor, CPTMS exception. The M_w of iPB was in range from 4.5×10^4 to 20.4×10^4 g/mol by changing the structure of external donor. The

change of the molecular weight distribution was not obvious, which suggested the molecular weight distribution was correlated with Ziegler-Natta catalyst, but not directly with the external donor.

Polymer characterization

The analysis of ¹³C NMR spectrum

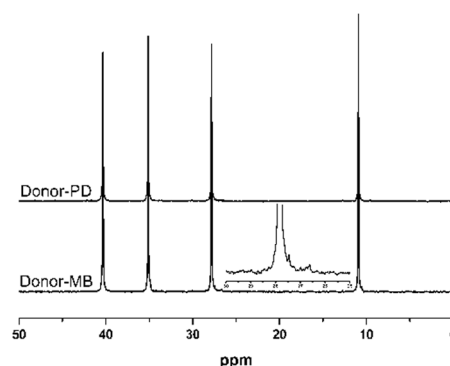


Fig. 2 ¹³C NMR spectra of iPB using different external donors

The high-temperature ¹³C NMR spectrum of the iPB was shown in Figure 2. There were four peaks in the aliphatic region. The peaks observed at $\delta=40.3$ and $\delta=34.8$ ppm had been assigned to the main chain carbons of iPB. The peak observed at $\delta=27.8$ ppm was assigned the side chain methylene carbon which directly bonded to the main chain of the isotactic iPB, the rest of peaks was belonged to the main chain of the atactic iPB. The peak observed at $\delta=11.0$ ppm was assigned to the methyl carbon in the ethylene side chain. Compared with iPB using Donor-PD, the iPB using Donor-MB had a large atactic iPB (the side chain methylene carbon which directly bonded to the main chain of the atactic iPB was appeared in 26-27ppm), which suggested the

Cite this: DOI: 10.1039/c0xx00000x

www.rsc.org/xxxxxx

ARTICLE TYPE

Table 2 The influences of external donors on the thermal performance of iPB

Samples (or Donor)	$T_m^a/^\circ\text{C}$	$\Delta H_m^b/(\text{J/g})$	$X_c^c\%$	$T_c^d/^\circ\text{C}$	$\Delta H_c^e/(\text{J/g})$	I.I. ^f (%)
Donor-MP	112.6	32.3	52.1	68.4	32.3	97.8
Donor-MB	111.2	29.3	47.3	62.9	31.8	96.4
Donor-MD	113.6	27.6	44.5	65.6	32.0	97.0
Donor-C	115.7	32.4	52.3	73.5	35.0	97.0
Donor-P	117.1	36.0	58.1	76.8	38.6	97.6
Donor-PB	116.9	35.2	56.7	75.6	37.1	98.0
Donor-PD	118.0	32.6	52.7	78.5	34.9	98.0
Donor-D	118.1	32.8	52.9	80.7	35.8	97.8
Donor-H	116.3	32.0	51.6	73.3	34.8	96.2
Donor-B	116.1	35.0	56.4	73.4	36.9	97.2
CPTMS	110.9	26.8	43.3	65.6	29.9	95.4

^a Melting temperature as determined from the peak maximum value in the endothermic curve of DSC. ^b The value of the endothermic enthalpy as determined from DSC. ^c The degree of crystallization calculated from the value of the endothermic enthalpy. ^d The crystallization temperature as determined from the exothermic curves of DSC. ^e The value of the endothermic enthalpy as determined from DSC. ^f The isotacticity of poly(1-butene).

stereoregularity of poly(1-butene) using the external donors with the large substituent groups were greater than the stereoregularity of poly(1-butene) using the external donor with the small substituent groups. The phenomenon was same as the results of isotactic index of iPB. According to the report of Proto and H-X. Zhang^{23, 24}, the stereospecificity of the catalyst system was affected by the structure of external donor and it was found that an increase of bulkiness of alkyl group had increased the isotactic. But because the stereoregularity of the obtained iPB was higher, the content of atactic iPB was very low, so the intent of peak of atactic structure was very weak, and the instrumental resolution was lower. Therefore, the stereoregularity of iPB was difficult to be accurately calculated from ¹³C NMR.

The thermal and crystallization behaviors of iPB

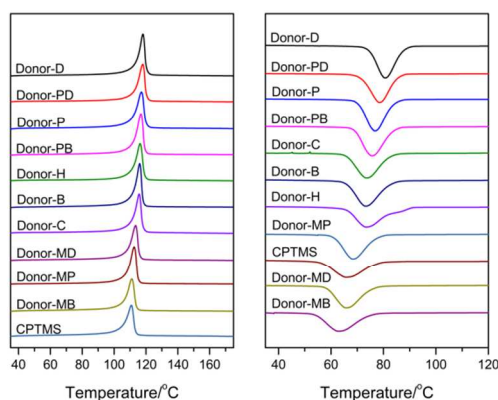


Fig. 3 The DSC melting curves and crystallization curves of iPB using different external donors

The thermal and crystallization behaviors of iPB were studied by differential scanning calorimetry.

The DSC results of poly(1-butene) are shown in Fig.3 and Table 2. As can be seen from Fig.3 and Table 2, the melting temperature and crystallization temperature of the prepared iPB showed a trend of increasing with the increase of the steric hindrance of substituent group of external donors. But when the steric hindrance of substituent group of external donors was too large, the melting point of the obtained iPB decreased to some extent with the increase of the steric hindrance of substituent group of external donors. For example, the melting temperature of iPB using Donor-H was 116.3°C which was lower than that of iPB using Donor-D and was higher than that of iPB using Donor-C. When external donor was Donor-D, the melting temperature could be reached to 118.1°C and the crystallization temperature could be reached to 80.7°C.

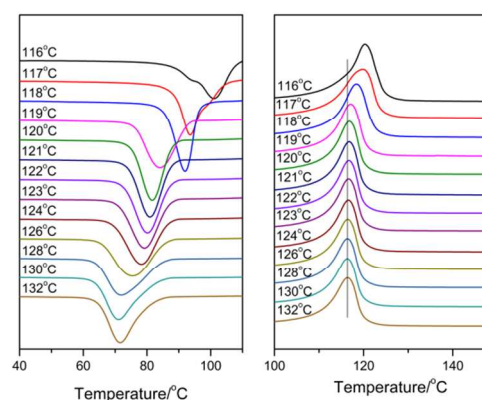


Fig. 4 The DSC crystallization and melting curve after different annealing temperature

Fillon et al.¹⁹ studied the self-nucleation behavior of iPP through the self-annealing procedures by DSC and the self-annealing temperature range divided into three domains. In Domain I or

“complete melting Domain”, the crystallization temperature (T_c) upon cooling from T_s remains constant and no self-nucleation can be detected. Domain II or “self-nucleation Domain” occurs when heat treatment at T_s caused a shift in crystallization temperature to higher temperatures with decreasing self-nucleation temperature. Finally, in Domain III or “self-nucleation and annealing Domain”, annealing and self-nucleation took place simultaneously¹⁰.

The crystallization and melting curves of SN at different annealing temperature of the Donor-P as an example were studied, as shown in Fig.4. As compared to the standard crystallization temperature obtained at the T_s temperature of 132°C, the crystallization temperature obtained at T_s temperature from 128°C to 132°C was not changed, indicating that the nucleation density of the samples remained constant in Domain I and the crystallization, nucleation, or aggregation of poly(1-butene) macromolecules did not occur^{11, 25}. When T_s was 126°C and remained constant at 126°C for 5min, self-nucleation of poly(1-butene) occurred, its crystallization temperature was shifted to higher temperature. That's because the unmelted component of poly(1-butene) could induced self-nucleation in the process, which could reduce the energy barrier of crystallization. Fig.4 showed that the melting peak increased obviously when the T_s temperature was 118°C, which because showing poly(1-butene) began self-nucleation and annealing, which suggested that the sample remain in Domain III. When the annealing temperature was lower than 119°C, the crystallization peaks became wider and the lamellae started to grow thick. The nucleation behavior of Donor-P illustrated that the minimum annealing temperature was 119°C. The optimal annealing temperature T_s of each sample was tested as above self-nucleation experiments and the results are listed in Table 3.

Table 3 Domain- II and optimal range of T_s of each sample

Samples	Domain- I	Domain- II	Domain-III	$T_s/^\circ\text{C}$
Donor-MP	$T_s > 126$	$116 < T_s < 126$	$T_s \leq 116$	116
Donor-MB	$T_s > 126$	$115 < T_s < 126$	$T_s \leq 115$	115
Donor-MD	$T_s > 127$	$117 < T_s < 127$	$T_s \leq 117$	117
Donor-C	$T_s > 127$	$119 < T_s < 127$	$T_s \leq 119$	119
Donor-P	$T_s > 127$	$119 < T_s < 127$	$T_s \leq 119$	119
Donor-PB	$T_s > 128$	$120 < T_s < 128$	$T_s \leq 120$	120
Donor-PD	$T_s > 130$	$119 < T_s < 130$	$T_s \leq 119$	119
Donor-D	$T_s > 128$	$120 < T_s < 128$	$T_s \leq 120$	120
Donor-H	$T_s > 128$	$119 < T_s < 128$	$T_s \leq 119$	119
Donor-B	$T_s > 128$	$119 < T_s < 128$	$T_s \leq 119$	119
CPTMS	$T_s > 125$	$115 < T_s < 125$	$T_s \leq 115$	115

The study of SSA experimental parameters

Effect of annealing time on the self-nucleation behavior of poly(1-butene)

DSC thermal history was memory of the previous crystal structure of the molten polymer. It was reported that the thermal historical memory could reduce when the annealing time increased^{19, 26, 27}. Therefore, we only studied the effect of different annealing time upon SN behavior of sample Donor-P when the annealing temperature was 119°C. The results are shown in Fig.5 and Table 4. When the annealing time was $t_s=0$, the crystallization temperature T_c (~88.9°C) was higher than the crystallization temperature of standard cooling. With the

increasing of the annealing time, the crystallization temperature gradually decrease. But the crystallization temperature was always higher than the crystallization temperature of standard cooling. The result revealed that increasing shorter annealing time couldn't effectively eliminate the relevant thermal historical memory when the annealing temperature was 119°C.

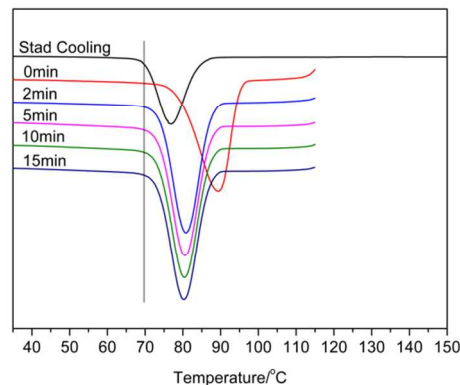


Fig. 5 The crystallization behavior of SN under different annealing time of sample Donor-P

Table 4 The crystallization behavior of SN under different annealing time of sample Donor-P

t_s/min	$T_c/^\circ\text{C}$	$\Delta H_c/(\text{J/g})$
Std-cooling	76.77	41.32
0	89.44	38.73
2	80.78	36.60
5	80.51	37.04
10	80.34	36.56
15	80.33	36.94

Fig.6 shows the effect of annealing time on the SSA melting curve at sample Donor-P. With the increase of the annealing time, the separation of melting peak becomes clearly and the melting peak increased. When the annealing time was 10min, it could not only effectively eliminate the effect of thermal history, but also the separation of melting peak was better.

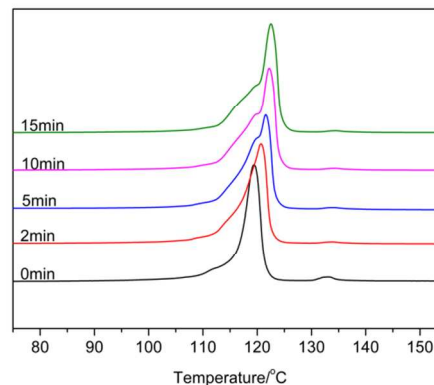


Fig. 6 The SSA melting curve under different annealing time t_s of sample Donor-P, DSC heating and cooling rates performed at 20°Cmin^{-1} . The annealing temperature of five steps was 120°C , 115°C , 110°C , 105°C and

100°C

Effect of the heating and cooling rates on the SSA behavior of poly(1-butene)

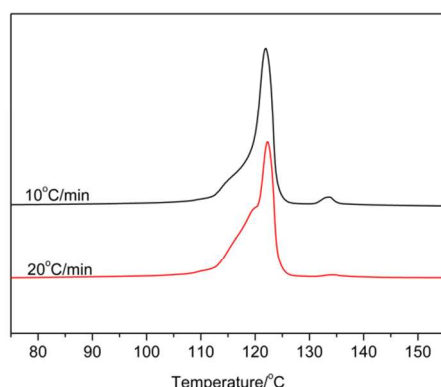


Fig. 7 The SSA melting curve under different heating and cooling rates of sample Donor-P

Pijpers et al.²⁸ have introduced high speed calorimetry concepts that could be advantageously applied to thermal fractionation experiments. The concepts showed that the increment in heating rates has been compensated by reducing sample mass. Based on the study of Lorenzo¹⁸, the weight of DSC sample was selected 3mg. Fig.7 shows the SSA melting curve under the two different heating and cooling rates of sample Donor-P at the annealing temperature $T_s=119^\circ\text{C}$ and annealing time $t_s=10$ min. As can be seen from the Fig.7, the thermal fractionation of the different heating and cooling rates (10°C/min and 20°C/min) was very similar. For low temperature melting peak, the effect of the thermal fractionation at 20°C/min was better than 10°C/min. It will appear a higher melting peak at two different heating and cooling rates, and the melting temperature (134.5°C) at 20°C/min slightly above the melting temperature (133.7°C) at 10°C/min. For poly(1-butene), the heating and cooling rate of 20°C/min could be either complete the SSA thermal fractionation or save test time.

Influence of the annealing temperature interval on SSA experiments of poly(1-butene)

In the SSA thermal fractionation process, the annealing temperature interval had a major impact on thermal analysis of polymers. Müller²⁵ reported that an appropriate annealing interval was favorable to obtain better thermal fractionation. Fig.8 showed the SSA melting curve under of the width of the fractionation window of sample PB-4 when annealing temperature was 119°C, annealing time was 10min and heating and cooling rate was 20°C/min. When the annealing temperature interval was 3°C, the low isotactic sequence of the chain segments in the annealing period was not crystallization, leading to incomplete separation. When the annealing temperature interval was 5°C, the resolution significantly increased, the separation of low temperature component was clearly. But when the annealing temperature interval continued to increase, the resolution decreased. It was because the rate of crystallization was fast, the crystallization was incomplete.

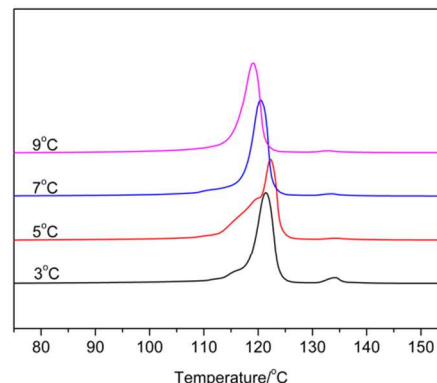


Fig.8 The SSA melting curve under of the width of the fractionation window of sample Donor-P

The above results showed that the different parameters of SSA have the important influence on the SSA thermal fractionation process. We first determined the annealing temperature of different samples. In order to better analyze the SSA, we selected the annealing time was 10min, the annealing temperature interval was 5°C and the heating and cooling rates was 20°C/min based on the results of SN experiment.

Application of SSA to research the sequence length

distribution of poly(1-butene) using different external donor

Accurate characterization of the sequence length distribution of poly(1-butene) could contribute to better understanding of the structure and properties of poly(1-butene). The crystallization behavior of poly(1-butene) was studied by the SSA thermal fractionation technology. The melting curves of iPB after SSA treatment were shown in Fig.9. Each peak of the melting point and the enthalpy of fusion ΔH_m were listed in Table 5. When R_1 was methyl in $R_1R_2\text{Si}(\text{OMe})_2$, the enthalpy of fusion ΔH_m of poly(1-butene) raze from 36.7 J/g to 44.8 J/g, which increased with the increasing of volume of R_2 substituent on alkoxy silanes. For other poly(1-butene) the phenomenon in accord with above rules, except for poly(1-butene) with Donor-H. It might be because right volume of hydrocarbon substituents on alkoxy silanes were conducive to the coordination between alkoxy silane donors and the active center, but too bulky hydrocarbon substituents on alkoxy silanes could prevent the coordination, the catalyst activity reduced, the content of ash of the poly(1-butene) increased, which lead to the high enthalpy of fusion ΔH_m .

In order to quantitatively evaluate the variations of each peak, the isotactic sequence length and distribution of poly(1-butene) were calculated by Peakfit 4.12 software. Fig.9 showed the SSA melting curve of poly(1-butene) and its fitted curves of sample by using Peakfit 4.12 software. The SSA results and the relative contents of all peaks on the SSA curve of poly(1-butene) were presented in Table 5. It has proved that the higher melting temperature on the SSA melting curves was corresponding to the higher isotacticity and isotactic sequence length in the molecular chains²⁹. As can be seen from Table 5, there were not peak 1 in

Cite this: DOI: 10.1039/c0xx00000x

www.rsc.org/xxxxxx

ARTICLE TYPE

Table 5 The SSA results of poly(1-butene) samples

Samples	I.I%	$T_g/^\circ\text{C}$	$\Delta H_m/(\text{J/g})$	$T_{m1}/^\circ\text{C}$	$n_1(\%)$	$T_{m2}/^\circ\text{C}$	$n_2(\%)$	$T_{m3}/^\circ\text{C}$	$n_3(\%)$
Donor-C	97.0	119	44.8	134.0	2.0	120.5	78.6	115.4	19.5
Donor-MD	97.0	117	44.5	133.1	1.3	120.2	81.1	114.9	17.6
Donor-MP	97.8	116	40.6	132.1	2.1	119.1	86.2	113.7	11.7
Donor-MB	96.4	115	36.7			118.9	85.3	114.7	14.7
Donor-PD	98.0	119	47.0	133.8	3.4	121.9	81.0	117.9	15.7
Donor-P	97.6	119	43.7	134.1	2.4	122.0	67.0	117.3	30.5
Donor-PB	98.0	120	43.9	134.3	2.8	122.4	78.1	118.1	19.1
Donor-MP	97.8	116	40.6	132.1	2.1	119.1	86.2	113.7	11.7
Donor-D	97.8	120	46.2	134.0	2.7	122.1	81.0	117.6	16.4
Donor-PD	98.0	119	47.0	133.8	3.4	121.9	81.0	117.9	15.7
Donor-MD	97.0	117	44.5	133.1	1.3	120.2	81.1	114.9	17.6
CPTMS	95.4	115	37.5			118.1	84.9	112.6	15.1
Donor-P	97.6	119	43.7	134.1	2.4	122.0	67.0	117.3	30.5
Donor-D	97.8	120	46.2	133.9	2.7	122.1	81.0	117.6	16.4
Donor-H	96.2	119	48.0	133.5	1.3	122.1	74.3	117.6	24.4
Donor-B	97.2	119	46.1	134.0	1.8	122.4	74.8	117.6	23.4

the melting curves of poly(1-butene) prepared by Donor-MB and CPTMS, indicating that the highest isotactic sequence length of poly(1-butene) prepared by Donor-MB and CPTMS were lower than those prepared by other donors. It might be because the smaller volumes of substituents on Donor-MB and CPTMS were, causing the absence of the highest isotactic active centers in the catalytic system with two donors. In the SSA melting curve of poly(1-butene), the mainly melting curves of poly(1-butene) was peak 2, and when the substituents on external donor was smaller, the melting temperature was lower than 120°C , such as Donor-MP, Donor-MB and CPTMS. The rest of peak 2 of poly(1-butene) was higher than 120°C , and the melting temperature was closer, indicating that the higher substituent was conducive to obtain high-performance poly(1-butene). The SSA results show that with the increasing of the steric hindrance of external donor, the melting temperature of iPB presented increase trend. For example, when R_1 was methyl in $R_1R_2\text{Si}(\text{OMe})_2$, with the increasing of the hindrance of R_2 , the melting temperature of peak 1 increase gradually from 132.1°C to 134°C ; the melting temperature of peak 2 and peak 3 increase, which showed that the sequence lengths of iPB gradually increase. When R_1 and R_2 was same substituents, the melting temperature was similar, but the relative contents of all peaks on the SSA curve of poly(1-butene) was difference. The SSA results of iPB using Donor-PD and Donor-D were similar and better other poly(1-butene), but the isotactic index and catalyst activity of iPB using Donor-PD was superior to that of iPB using Donor-D. Therefore, Donor-PD had better advantage relative to other external donors in the polymerization of 1-butene.

Table 6 The lamellar thicknesses of poly(1-butene) samples after SSA thermal fractionation

Samples	L_1/nm	L_2/nm	L_3/nm
Donor-C	24.68	3.32	2.50
Donor-MD	17.28	3.26	2.45
Donor-MP	12.96	3.05	2.31
Donor-MB		3.01	2.42
Donor-PD	22.54	3.65	2.85
Donor-P	25.92	3.68	2.76
Donor-PB	28.80	3.78	2.88
Donor-MP	12.96	3.05	2.31
Donor-D	24.68	3.70	2.80
Donor-PD	22.54	3.65	2.85
Donor-MD	17.28	3.26	2.45
CPTMS		2.88	2.21
Donor-P	25.92	3.68	2.76
Donor-D	23.56	3.70	2.80
Donor-H	19.94	3.70	2.80
Donor-B	24.68	3.78	2.80

The lamellar thickness can be estimated from the SSA results with Thomson-Gibbs equation^{12, 30}.

$$T_m = T_m^o \left(1 - \frac{2\sigma}{\Delta H_o L_i} \right)$$

Where $T_m^o=409.25\text{K}$ (equilibrium melting temperature), $\Delta H_o=1.35 \times 10^8\text{J/m}^3$, $\sigma=17.1 \times 10^{-3}\text{J/m}^2$ (surface energy) and L_i is the lamellar thickness³¹. The lamellae thickness of iPB after SSA thermal fractionation was calculated and listed in Table 6. When

R_1 was methyl in $R_1R_2Si(OMe)_2$, with the increasing of the steric hindrance of R_2 , the lamellae thickness of iPB gradually increased. But when R_1 was isopropyl, the lamellae thickness of iPB using Donor-P, Donor-PD and Donor-PB, which was higher than the lamellae thickness of iPB using Donor-MP. The lamellae thickness of iPB prepared using Donor-PB was the thickest (the lamellar thickness of peak 1 was 28.80nm, the lamellar thickness of peak 2 was 3.78nm, the lamellar thickness of peak 3 was 2.88nm). When R_1 and R_2 was same substituent, the lamellae thickness of peak 2 and peak 3 was same, but the lamellae thickness of peak 1 was different, and the thickest lamellae thickness of peak 1 of iPB using Donor-P was 25.92.

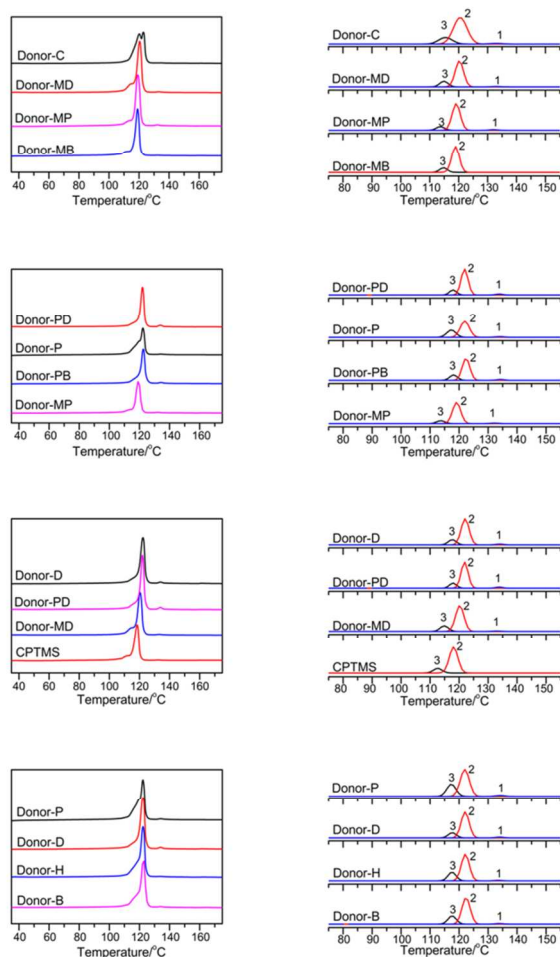


Fig.9 The SSA melting curve of poly(1-butene) and its fitted curves of sample by using Peakfit 4.12 software

Moreover, in order to further the analysis, we introduce the terms of “arithmetic average L_n ”, the “weighted average L_w ”, and the broadness index L_w/L_n ³².

$$L_n = \frac{n_1L_1 + n_2L_2 + \dots + n_jL_j}{n_1 + n_2 + \dots + n_j} = \sum f_i L_i$$

$$L_w = \frac{n_1L_1^2 + n_2L_2^2 + \dots + n_jL_j^2}{n_1L_1 + n_2L_2 + \dots + n_jL_j} = \sum f_i L_i^2$$

$$I = \frac{L_w}{L_n}$$

where n_i was the normalized peak area, and the L_i was the lamellar thickness for each fraction. The results of all samples are listed in Table 7. As can be seen from Table 7, when R_1 was methyl in $R_1R_2Si(OMe)_2$, with the increasing of the steric hindrance of R_2 , the L_n , n_w and I increases gradually. But when R_1 was isopropyl, the varied tendency of the L_n , n_w and I doesn't show the regularity. It is found that iPB prepared using Donor-PB has the highest isotactic component and the lower medium component relative to other iPB, but the amount of the medium component was higher, therefore, the sequence length distribution was broader.

Table 7 Lamellar thickness statistical parameters of iPB samples prepared by the different external donors

Samples	L_w /nm	L_n /nm	$I=L_w/L_n$
Donor-C	6.15	3.59	1.71
Donor-MD	4.11	3.30	1.25
Donor-MP	3.84	3.17	1.21
Donor-MB	2.94	2.92	1.01
Donor-PD	7.03	4.17	1.69
Donor-P	7.00	3.93	1.78
Donor-PB	8.35	4.31	1.94
Donor-MP	3.84	3.17	1.21
Donor-D	7.00	4.12	1.70
Donor-PD	7.03	4.17	1.69
Donor-MD	4.11	3.30	1.25
CPTMS	2.80	2.78	1.01
Donor-P	7.00	3.93	1.78
Donor-D	6.69	4.09	1.64
Donor-H	4.67	3.69	1.27
Donor-B	5.98	3.93	1.52

Conclusions

In this paper, poly(1-butene) was prepared by Ziegler-Natta catalysts using silane external donor. The influence of steric hindrance of external donor on the structure of poly(1-butene) was studied by DSC and ¹³C NMR. The crystallization behavior and sequence length distribution of poly(1-butene) samples were studied by the successive self-nucleation and annealing calorimetric technique. It was found that the proper annealing time t_s , annealing temperature interval and heating and cooling rates could enhance the separation of the different crystalline components. The results showed that iPB has higher isotacticity and stereoregularity by the bulk polymerization. The SSA results showed the melting temperature of iPB increased with the increasing of the steric hindrance of external donor, the subtle differences in the temperature has a big impact on the lamellae thickness of iPB. When R_1 was methyl in $R_1R_2Si(OMe)_2$, the L_n , n_w and I increased gradually with increasing of the steric hindrance of R_2 . But, when R_1 was isopropyl, the tendency of the L_n , n_w and I had no regularity.

Acknowledgements

The authors gratefully acknowledge the financial supports provided by the National Natural Science Foundation of China (No. 51073170, 50703044, 51403216)

5

Notes and references

^a College of Chemistry and Chemical Engineering, University of Chinese Academy of Sciences, Beijing, China. Fax: 010 88256321; Tel: 010 88256321; E-mail: zhangly@ucas.ac.cn

- ¹⁰ ^b Beijing National Laboratory for Molecular Science, Key Laboratory of Engineering Plastics, Institute of Chemistry, Chinese Academy of Sciences, China; Fax: 010 62562697; Tel: 010 62562697; E-mail: lihuayi@iccas.ac.cn
- 15 1. L. Luciani, J. Seppala and B. Lofgren, *Prog Polym Sci*, 1988, **13**, 37-62.
 2. P. M. Cham, T. H. Lee and H. Marand, *Macromolecules*, 1994, **27**, 4263-4273.
 3. G. Natta, P. Pino, P. Corradini, F. Danusso, E. Mantica, G. Mazzanti and G. Moraglio, *J Am Chem Soc*, 1955, **77**, 1708-1710.
 - 20 4. G. Natta, *J Polym Sci*, 1955, **16**, 143-154.
 5. J. B. Diao, Q. Wu and S. G. Lin, *J Polym Sci Pol Chem*, 1993, **31**, 2287-2293.
 6. S. Kojoh, T. Tsutsui, N. Kashiwa, M. Itoh and A. Mizuno, *Polymer*, 1998, **39**, 6309-6313.
 - 25 7. Z. S. Fu, S. T. Tu and Z. Q. Fan, *Ind Eng Chem Res*, 2013, **52**, 5887-5894.
 8. V. Busico, R. Cipullo, G. Monaco, G. Talarico, M. Vacatello, J. C. Chadwick, A. L. Segre and O. Sudmeijer, *Macromolecules*, 1999, **32**, 4173-4182.
 - 30 9. M. L. Arnal, V. Balsamo, G. Ronca, A. Sanchez, A. J. Muller, E. Canizales and C. U. de Navarro, *J Therm Anal Calorim*, 2000, **59**, 451-470.
 10. A. T. Lorenzo, M. L. Arnal, A. J. Muller, A. B. de Fierro and V. Abetz, *Eur Polym J*, 2006, **42**, 516-533.
 - 35 11. A. T. Lorenzo, M. L. Arnal, J. J. Sanchez and A. J. Muller, *J Polym Sci Pol Phys*, 2006, **44**, 1738-1750.
 12. H. F. Chang, Y. Zhang, S. T. Ren, X. F. Dang, L. Y. Zhang, H. Y. Li and Y. L. Hu, *Polym Chem-Uk*, 2012, **3**, 2909-2919.
 13. O. Kudinova, V. Krashennnikov, L. Novokshonova, T. Kron and E. Petrov, *Dokl Chem*, 2008, **423**, 309-309.
 - 40 14. H. G. Ren, M. Yang, B. J. Zhang, X. F. Ren, B. Y. Liu, Y. J. Wang and I. Kim, *Macromol Res*, 2012, **20**, 985-989.
 15. D. Cavallo, L. Gardella, G. Portale, A. J. Muller and G. C. Alfonso, *Polymer*, 2014, **55**, 137-142.
 - 45 16. A. J. Muller, Z. H. Hernandez, M. L. Arnal and J. J. Sanchez, *Polym Bull*, 1997, **39**, 465-472.
 17. M. L. Arnal, J. J. Sanchez and A. J. Muller, *Polymer*, 2001, **42**, 6877-6890.
 18. A. T. Lorenzo, M. L. Arnal, A. J. Muller, A. B. de Fierro and V. Abetz, *Macromol Chem Phys*, 2006, **207**, 39-49.
 - 50 19. B. Fillon, J. C. Wittmann, B. Lotz and A. Thierry, *J Polym Sci Pol Phys*, 1993, **31**, 1383-1393.
 20. J. V. Seppala and M. Harkonen, *Makromol Chem*, 1989, **190**, 2535-2550.
 - 55 21. M. Harkonen and J. V. Seppala, *Makromol Chem*, 1991, **192**, 2857-2863.
 22. X. R. Shen, Z. S. Fu, J. Hu, Q. Wang and Z. Q. Fan, *J Phys Chem C*, 2013, **117**, 15174-15182.
 23. H. X. Zhang, Y. J. Lee, J. R. Park, D. H. Lee and K. B. Yoon, *Macromol Res*, 2011, **19**, 622-628.
 - 60 24. A. Proto, L. Oliva, C. Pellecchia, A. J. Sivak and L. A. Cullo, *Macromolecules*, 1990, **23**, 2904-2907.
 25. A. J. Muller and M. L. Arnal, *Prog Polym Sci*, 2005, **30**, 559-603.
 26. M. Y. Keating and E. F. Mccord, *Thermochim Acta*, 1994, **243**, 129-145.
 - 65 27. M. V. Massa, M. S. M. Lee and K. Dalnoki-Veress, *J Polym Sci Pol Phys*, 2005, **43**, 3438-3443.
 28. T. F. J. Pijpers, V. B. F. Mathot, B. Goderis, R. L. Scherrenberg and E.

- W. van der Vegte, *Macromolecules*, 2002, **35**, 3601-3613.
- 70 29. J. Kang, F. Yang, T. Wu, H. L. Li, Y. Cao and M. Xiang, *Eur Polym J*, 2012, **48**, 425-434.
 30. V. Virkkunen, P. Laari, P. Pitkanen and F. Sundholm, *Polymer*, 2004, **45**, 4623-4631.
 31. M. Yamashita and T. Takahashi, *Polym J*, 2008, **40**, 996-1004.
 - 75 32. M. Keating, I. H. Lee and C. S. Wong, *Thermochim Acta*, 1996, **284**, 47-56.

GRAPHICAL ABSTRACT

Application of successive self-nucleation and annealing (SSA) to poly(1-butene) prepared by Ziegler-Natta catalysts with different external donors

Tao Zheng, Qian Zhou, Qian Li, Huayi Li, Liaoyun Zhang, Youliang Hu

The SSA thermal fractionation technology could analysis the accurate characterization of the sequence length distribution of iPB.

